

# Understanding the Glass-Forming Ability of Active Pharmaceutical Ingredients for Designing Supersaturating Dosage Forms

KOHSAKU KAWAKAMI,<sup>1</sup> TOSHINORI USUI,<sup>2</sup> MITSUNARI HATTORI<sup>2</sup>

<sup>1</sup>International Center for Materials Nanoarchitectonics (WPI-MANA), National Institute for Materials Science, Tsukuba, Ibaraki 305-0044, Japan

<sup>2</sup>Mettler-Toledo K.K., Taito-ku, Tokyo 110-0008, Japan

Received 30 January 2012; revised 15 March 2012; accepted 5 April 2012

Published online 24 April 2012 in Wiley Online Library (wileyonlinelibrary.com). DOI 10.1002/jps.23166

**ABSTRACT:** Amorphous solid dispersions have great potential for enhancing oral absorption of poorly soluble drugs. Crystallization behavior during storage and after exposure to aqueous media must be examined in detail for designing stable and effective amorphous formulations, and it is significantly affected by the intrinsic properties of an amorphous drug. Many attempts have been made to correlate various thermodynamic parameters of pharmaceutical glasses with their crystallization behavior; however, variations in model drugs that could be used for such investigation has been limited because the amorphous characteristics of drugs possessing a high crystallization tendency are difficult to evaluate. In this study, high-speed differential scanning calorimetry, which could inhibit their crystallization using high cooling rates up to 2000°C/s, was employed for assessing such drugs. The thermodynamic parameters of the glasses, including glass transition temperature ( $T_g$ ) and fragility, were obtained to show that their crystallization tendency cannot be explained simply by the parameters, although there have been general thought that fragility may be correlated with crystallization tendency. Also investigated was correlation between the thermodynamic parameters and crystallization tendency upon contact with water, which influences *in vivo* efficacy of amorphous formulations.  $T_g$  was correlated well with the crystallization tendency upon contact with water. © 2012 Wiley Periodicals, Inc. and the American Pharmacists Association *J Pharm Sci* 101:3239–3248, 2012

**Keywords:** thermal analysis; amorphous; crystallization; physical stability; glass-forming ability; glass transition; fragility; high-speed DSC

## INTRODUCTION

Amorphous solid dispersions are one of the most promising options for developing poorly soluble drugs because the amorphous state has solubility advantage over crystals.<sup>1–3</sup> The maintenance of high-level supersaturation after dissolution is important for improving oral absorption.<sup>3–5</sup> However, many problems remain unsolved for active use of solid dispersions as oral dosage forms. For example, special facilities are required for manufacturing amorphous formulations. Commercial production currently employs either a spray-drying<sup>6</sup> or hot-melt extrusion.<sup>7</sup> Although

spray drying is a well-established technique in industry, special facilities are required to allow handling of flammable solvents used for dissolving poorly soluble drugs. Another serious problem is the absence of protocols for predicting the physical stability of amorphous formulations,<sup>1,3,8,9</sup> mainly because the temperature dependence of the nucleation rate is difficult to evaluate. An accurate estimation of the crystallization rate during storage can be performed only by observing the stability at the same temperature with the storage conditions. Thus, efforts are ongoing to establish a protocol for predicting the long-term physical stability of amorphous formulations.<sup>8,9</sup>

Failure of a liquid to crystallize below the melting temperature had been explained only by kinetics. In the pharmaceutical field, the amorphous state has widely been believed to be maintained stably below a temperature lower 50°C or more than a glass

Correspondence to: Kohsaku Kawakami (Telephone: +81-29-860-4424; Fax: +81-29-860-4708; E-mail: kawakami.kohsaku@nims.go.jp)

*Journal of Pharmaceutical Sciences*, Vol. 101, 3239–3248 (2012)  
© 2012 Wiley Periodicals, Inc. and the American Pharmacists Association

transition temperature ( $T_g$ ), where configurational entropy almost disappears. Recently, frustration in liquid structure is gaining considerable attention as an important factor in the inhibition of crystallization, in which a difference in the locally favored liquid structure and crystal structure is considered to play a crucial role.<sup>10–12</sup> Under this assumption,  $T_g$  cannot predict the glass-forming ability and, as a matter of fact, principal component analysis showed that the ability to form a stable amorphous state depends instead on the molecular weight and the complexity of the molecular structure.<sup>13</sup> Glass-forming ability is an important notion for evaluating possibility of amorphous formulations because drugs with low glass-forming ability must be stabilized using a large amount of excipients miscible with the drug.

Determining factors that dominate the glass-forming ability is difficult partially because of the difficulty in evaluating the amorphous characteristics of compounds that crystallize easily. Variation in the data is always limited when the correlation between thermodynamic parameters and glass-forming ability is discussed. High-speed differential scanning calorimetry (DSC) is a novel tool that allows temperature change at a much faster rate compared with conventional DSC, which should make analysis of amorphous materials much easier. In this study, drugs with very low glass-forming ability, tolbutamide (TLB), carbamazepine (CBZ), and haloperidol (HPD), were employed as model compounds for evaluating amorphous characteristics using high-speed DSC.

Another interest of this study is the relevance of glass-forming ability in the dry state to crystallization tendency in the wet state. Drugs with a low crystallization tendency in the wet state are expected to be good candidates for amorphous formulations because maintenance of the supersaturated state can be expected. Transformation in the wet state can be explained by two mechanisms: solid–solid and solvent-mediated transformations. The likelihood of the former mechanism to occur in the transformation should be identical to crystallization tendency in the dry state, whereas the latter mechanism is believed to be governed by solubility and the interaction of the drug with solvents.<sup>14,15</sup> The solvent-mediated transformation in water is frequently faster than the transformation expected from the solubility,<sup>14</sup> and it is usually explained in terms of interactions between the solid and water via hydrogen bonding. Transformation in aqueous media is a very important process that requires understanding for the design of effective amorphous dosage forms. Crystallization tendency in the wet state is also discussed in relation to various amorphous characteristics.

## EXPERIMENTAL

### Materials

Tolbutamide (TLB) and indomethacin were obtained from Wako Pure Chemicals (Osaka, Japan). CBZ and HPD were obtained from Nacalai Tesque (Kyoto, Japan). Ketoconazole and itraconazole were obtained from Tokyo Chemical Industry (Tokyo, Japan). Acetaminophen and procaine were obtained from MP Biomedicals (Solon, Ohio). Nifedipine, fenofibrate, and ibuprofen were supplied from Alexis Biochemicals (San Diego, California), Sigma–Aldrich (St. Louis, Missouri), and Hamari Chemicals (Osaka, Japan), respectively. All the reagents were used as supplied.

### Thermal Stability of Model Drugs

A trace amount of impurity may affect the crystallization behavior. Thermal stability of each drug was investigated because degradation products may appear during the thermal analysis. All the compounds except CBZ and TLB were regarded as stable in the melt-crystallization cycle because the decrease in weight was below 0.01% in the thermogravimetry analysis on SDT Q600 (TA Instruments, New Castle, Delaware) up to their melting temperatures. Note that decrease in weight due to removal of adsorbed water was ignored in this evaluation. CBZ and TLB were annealed at 200°C and 140°C, respectively, on DSC Q2000 (TA Instruments) and dissolved by ethanol. High-performance liquid chromatography (HPLC) analysis was performed on a Shimadzu Prominence (Shimadzu, Kyoto, Japan) equipped with a Cosmosil 5C18-AR-II (150 mm L × 5.0 mm ID; Nacalai Tesque, Kyoto, Japan) with a flow rate at 1 mL/min. For CBZ, the column was equilibrated by acetonitrile–water (10:90), which was changed to 100:0 in 40 min, followed by elution using acetonitrile for 20 min. For TLB, acetonitrile–water (5:95) was applied for 5 min, followed by gradient to 100:0 in 45 min and elution by acetonitrile for 10 min. Detection wavelength and injection volume were 210 nm, and 2  $\mu$ L, respectively.

### Differential Scanning Calorimetry

Conventional DSC measurements were performed on DSC Q2000 (TA Instruments). The instrument was periodically calibrated with indium and sapphire. Nitrogen was supplied as an inert gas at a flow rate of 50 mL/min. Approximately 5 mg of samples was loaded in an aluminum-sealed pan. CBZ, HPD, and TLB were melted at 200°C, 170°C, and 140°C for 0.5 min, respectively, to obtain the amorphous state. All the measurements were duplicated to ensure reproducibility. Onset values are reported to present  $T_g$ .

## High-Speed DSC

High-speed DSC measurements were conducted on Flash DSC 1 (Mettler-Toledo, Greifensee, Switzerland). Approximately 100–400 ng of sample was loaded onto the central portion of a sensor using an optical microscope, and the sample mass was determined from the melting enthalpy during heating at 3°C/s. CBZ, HPD, and TLB were melted at 200°C, 170°C, and 140°C for 0.5 s, respectively, to obtain the amorphous state. One sensor was assigned to one compound, and each was calibrated by the manufacturer prior to the supply. After a series of experiments, the accuracy of the temperature was validated by measuring reference samples of indium and naphthalene. Nitrogen was supplied as an inert gas at a flow rate of 20 mL/min. All measurements were duplicated to ensure reproducibility. Onset values are reported to present  $T_g$ .

## Investigation of Crystallization Tendency in Wet State

Model drugs that have high and moderate glass-forming ability were investigated in this study. The model drugs were melted in open aluminum pans on SDT Q600 (TA Instruments), to which 100 mL/min of argon gas was supplied. Samples of approximately 10 mg were heated to above their melting temperatures at a rate of 10°C/min, followed by cooling in the air stream. Subsequently, 20  $\mu$ L of water was added to each sample in the pan, which was then allowed to stand at room temperature for 24 h. Aluminum lids with pinholes were placed on the sample pans for DSC measurements at 10°C/min on Q2000 (TA Instruments). Crystallinity was evaluated based on their melting enthalpy.

## RESULTS

### Thermal Stability of Model Drugs

Thermogravimetry analysis indicated that all the model drugs used in this study were thermally stable in the heat-cool cycles except CBZ and TLB as described in the Experimental section. 0.86 % decrease in weight was observed for CBZ by heating up to 200°C. In the HPLC analysis, CBZ was found at 17.1 min. The degradation products were not found for the sample annealed at 200°C for 1 min. However, a novel peak appeared at 23.4 min, of which the peak area corresponded to approximately 1% of CBZ, for the sample annealed for 10 min, indicating that long or repeated annealing above the melting temperature may cause degradation. Thus, the thermal program for melting CBZ was determined carefully for the following studies to avoid degradation. Although 0.02% decrease in weight was observed for TLB at 140°C in the thermogravimetry analysis, no degradation products were found for the sample that was annealed

at 140°C for 10 min in the HPLC analysis. Thus, a decrease in weight was likely to be due to partial vaporization of the melt.

### Conventional Thermal Analysis of the Model Drugs

Figure 1 shows the thermal behavior of the model drugs investigated on a conventional DSC. TLB used in this study was initially in form I, which undergoes enantiotropic polymorphic transition at 40°C,<sup>16</sup> followed by melting at 128°C. In subsequent cooling processes, exothermic peaks at about 60°C were observed and interpreted as crystallization. The crystallization peak decreased in size with increasing cooling rate; however, a small peak remained even when the sample was cooled at 20°C/min. A glass transition appeared at 4°C in the cooling curve and the subsequent heating curve, suggesting that TLB was partially transformed into the amorphous state during cooling at a rate of 20°C/min. CBZ was supplied as form III, which transformed into the most stable form, form I, via a melt-crystallization process at 179°C.<sup>17</sup> During the cooling process, crystallization curves were always observed and glass transition was not investigated in the subsequent heating curves, when the cooling rate was slower than 20°C/min. Note that the crystallization behavior in the cooling process at 5°C/min appeared to be different from those in the 10 and 20°C/min cooling curves, which may be due to production of a trace amount of degradation products during the temperature scan. The only thermal event for HPD was a melting peak at 150°C in the heating curve. In the subsequent cooling, a sharp crystallization exotherm was always observed at about 100°C, regardless of the cooling rate, and glass transition was not observed in any cooling/heating curves. Thus, in the conventional DSC-quenching procedure, TLB was partially transformed into the amorphous state, whereas CBZ and HPD crystallized easily and the amorphous state was not obtained. These observations revealed the difficulty in evaluating the amorphous characteristics of these drugs on a conventional DSC.

### Crystallization/Amorphization During Rapid Cooling

Figure 2 shows the effect of cooling rates on the thermal behavior of model drugs in the high-speed DSC analysis. Crystallization was not observed in the cooling curves for TLB and CBZ, even at the slowest cooling rate of 1°C/s. In the subsequent heating process,  $T_g$  was found at 23–27°C and 59–66°C, respectively, as indicated by arrows in the figures. The  $T_g$  value for CBZ agreed well with the reported value<sup>13</sup>; however, that of TLB was higher,<sup>13</sup> although little information is available because of the difficulty in obtaining the amorphous state. The dependence of  $T_g$  on the cooling rate can be elucidated in terms of difference in degree of relaxation, which decreases free

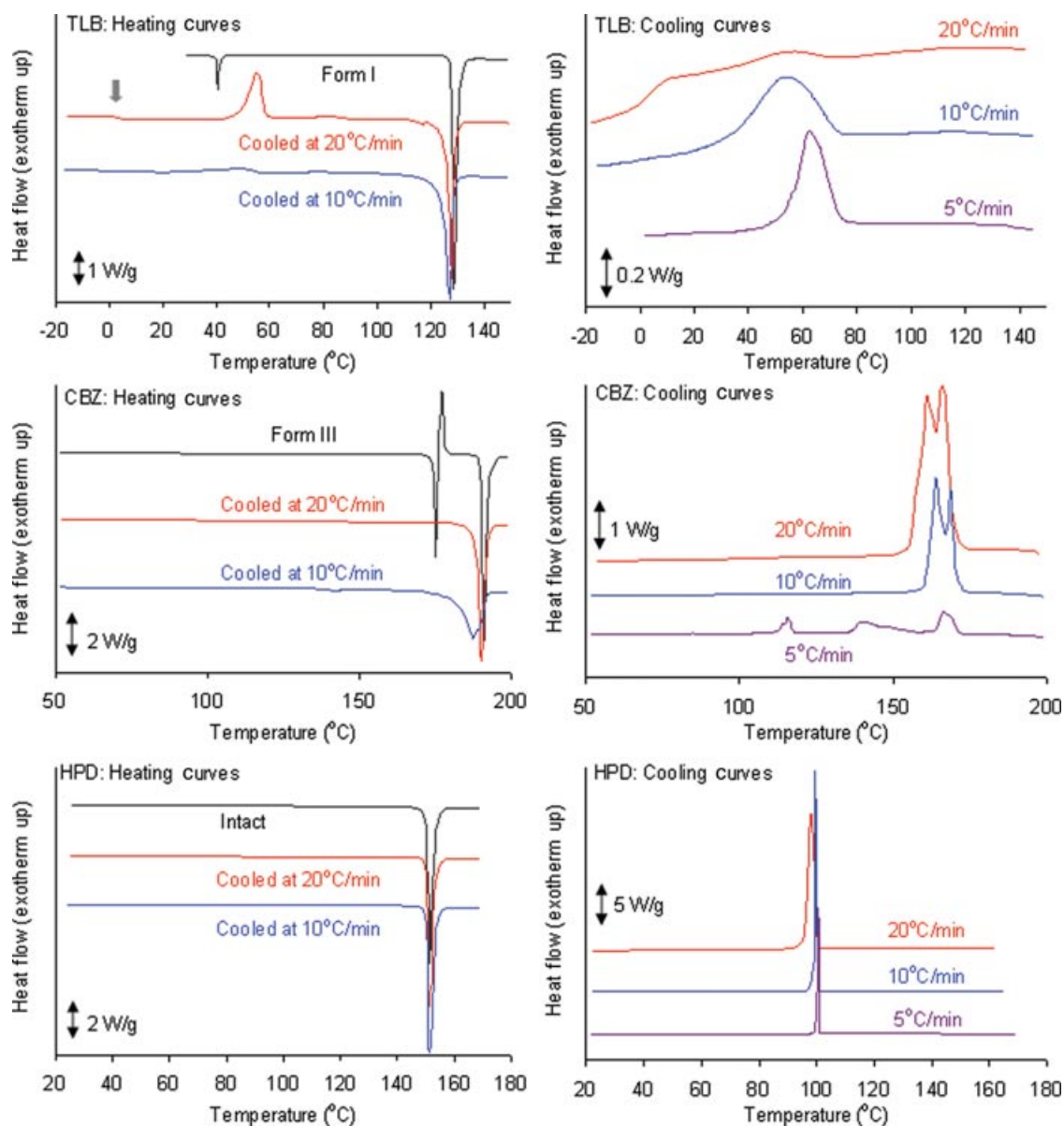


**Figure 1.** Heating (left)/cooling (right) curves of TLB, CBZ, and HPD obtained on a conventional DSC. Samples were melted by heating above the melting temperature at 10°C/min (top curves in left columns), followed by cooling at 20°C/min (top curves in right columns). Subsequently, two heating/cooling cycles were applied: heating at 10°C/min (middle curves of left columns), followed by cooling at 10°C/min (middle curves of right columns), and heating at 10°C/min (bottom curves of left columns), followed by heating at 5°C/min (bottom curves in right columns). Note that the heating processes after the cooling were initiated far below the lower temperature limits of the figures. An arrow in the figure indicates  $T_g$ .

volume and increases molecular cooperativity to raise  $T_g$ .<sup>18</sup> The absence of melting peaks indicated that these drugs were totally transformed into the amorphous state under all cooling rates presented. The crystallization temperature of HPD decreased with increasing cooling rate, and another exothermic peak appeared at 44°C in the cooling curves when HPD was cooled faster than 30°C/s. The hot crystallization peak completely disappeared at a cooling rate faster than 100°C/s.  $T_g$  was found at 27°C in the heating curves,

when the cooling rate was faster than 30°C/s. The endothermic peak at 44°C and the cold crystallization peak at 60°C grew with increasing cooling rate and exhibited a constant value above 100°C/s. The appearance of  $T_g$  indicates that the exothermic peak at 44°C in the cooling curves was not due to crystallization but to formation of a mesophase, which is supported by the observation that the peak was always found at the same temperature regardless of very wide range of the heating/cooling rate and direction of scan. These

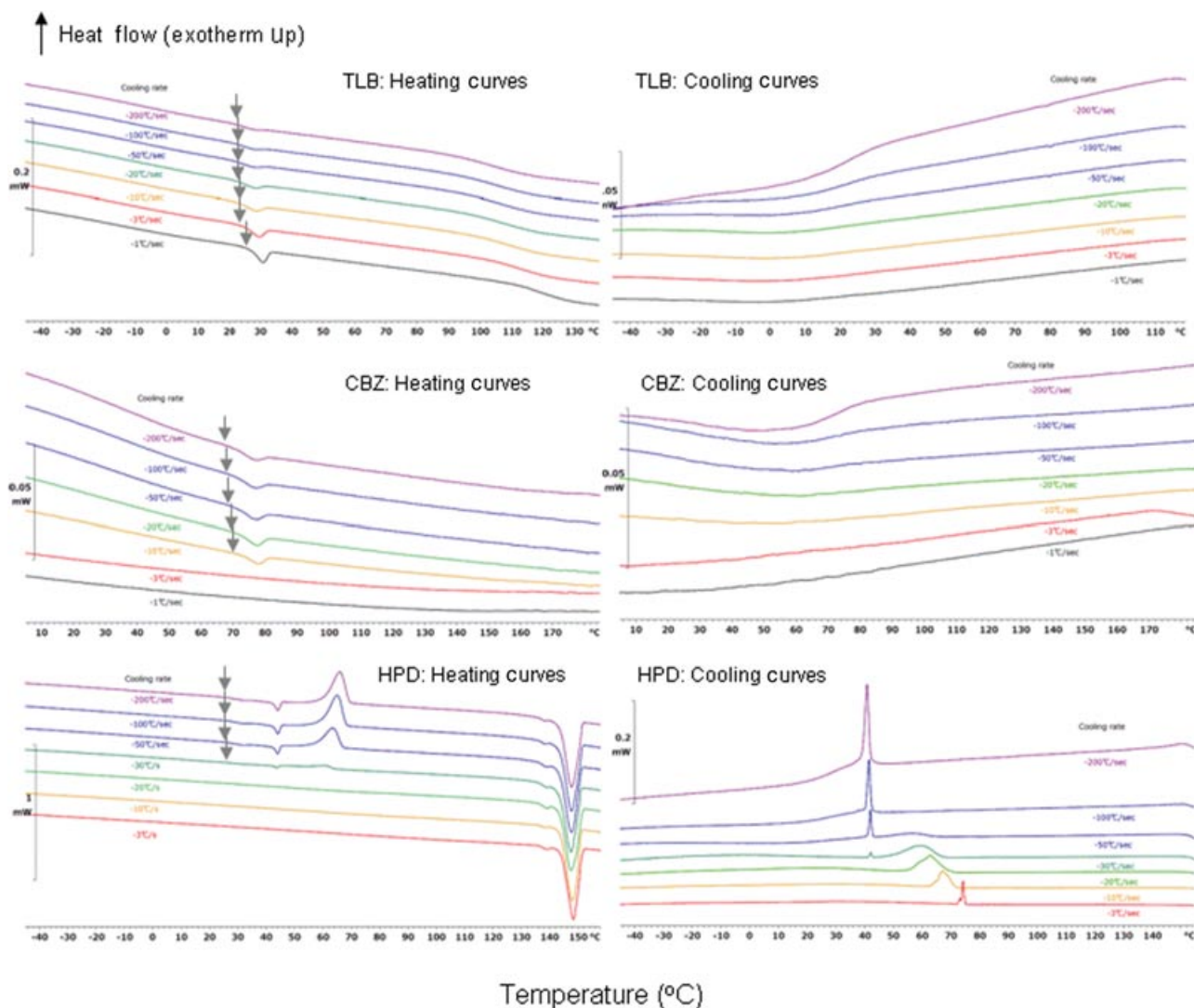


**Figure 2.** Heating (left)/cooling (right) curves of TLB, CBZ, and HPD obtained on a high-speed DSC. The experimental procedure was the same with that for Figure 1, except that high scan rates were applied. Samples were initially melted by heating above the melting temperature at 100°C/s (data not shown). Subsequently, samples were cooled at various cooling rates as shown in the figures (right curves) and heated at a constant rate, 100°C/s (left curves). Arrows in the figures indicate  $T_g$ s.

results suggest that HPD was transformed into the mesophase at cooling rates faster than 100°C/s.

### Determination of Fragility

Fragility is an important notion that may explain various amorphous characteristics, including the glass-forming ability.<sup>13,19</sup> Various methods are available for determining the fragility value,<sup>18,20</sup> among which the dependence of  $T_g$  on the ramp rate,  $q$ , in DSC measurements is the most suitable because it does not require precise thermodynamic parameters such as heat capacity. The fragility value,  $m$ , is determined using the following equations<sup>18,20</sup>:

$$m = \left. \frac{d \log \tau}{d(T_g/T)} \right|_{T=T_g} = \frac{1}{2.303 T_g} \frac{\Delta E_{T_g}}{R} \quad (1)$$

where

$$-\frac{\Delta E_{T_g}}{R} = \frac{d(\ln q)}{d(1/T_g)} \quad (2)$$

Thus,  $m$  can be determined from the dependence of  $T_g$  on the ramp rate.  $m$  is related with the strength parameter,  $D$ , as follows:

$$m = \frac{DT_0/T_g}{2.303(1 - T_0/T_g)^2} \quad (3)$$

A glass with a large  $D$  value ( $D > 30$ ) is considered as “strong,” whereas that with a low  $D$  value ( $D < 10$ ) is regarded as “fragile.” Figure 3 shows DSC curves of TLB heated at various ramp rates. The values for  $m$  and  $D$  of the TLB glass were 108 and 6.44,

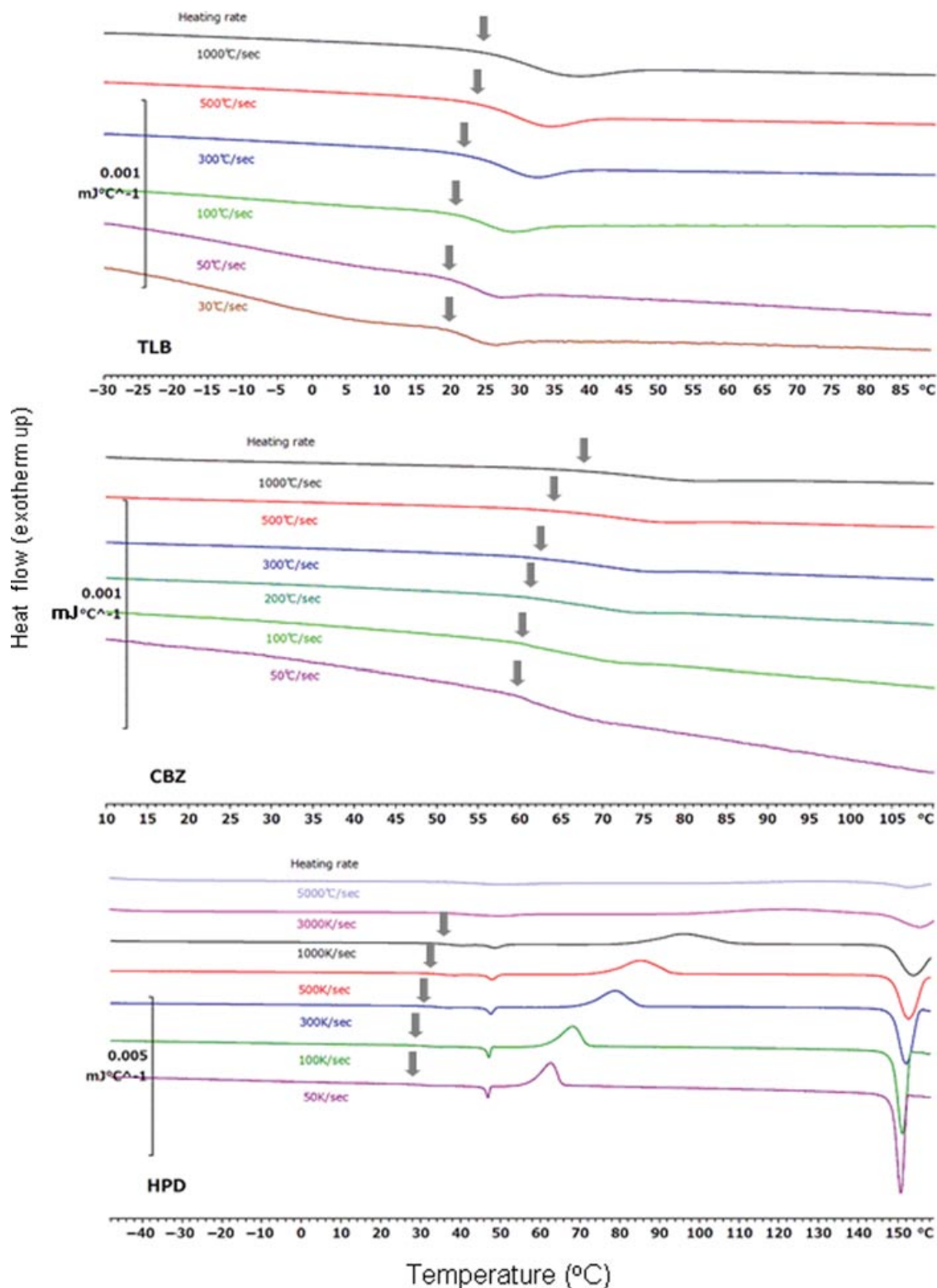


**Figure 3.** Effect of heating rate on  $T_g$ s of TLB, CBZ, and HPD. The cooling rates between each heating process were 2000  $^\circ\text{C}/\text{s}$  for CBZ and HPD, and 200  $^\circ\text{C}/\text{s}$  for TLB. Arrows in the figures indicate  $T_g$ s.

respectively. Those for CBZ glass were 55.3 and 15.0, respectively. For HPD,  $m$  and  $D$  of the mesophase (not the glassy phase) were 72.8 and 10.4, respectively. Thus, only the TLB glass could be regarded as fragile, whereas other glasses are considered to form relatively strong pharmaceutical glasses. Also, these  $m$  and  $D$  values are almost the same with those of the compounds with high glass-forming ability. This observation does not support the general thought that glasses with low glass-forming ability are fragile, which is in agreement with earlier investigation made by Baird et al.<sup>13,21</sup>

Fragility can be determined using various methods; however, the values obtained are sometimes affected by the procedure employed. It has frequently been pointed out that thermodynamic fragility does not correlate with dynamic fragility at least for small organic compounds.<sup>22,23</sup> The dynamic fragility can be determined by extrapolating configurational entropy to zero, or by estimating activation energy for molecular motion at  $T_g$  from the ramp rate dependence of  $T_g$  or width of the  $T_g$  range.<sup>18,20</sup> Thus, values from these methods should agree with each other only when the compound exhibits “ideal” fragile behavior. Employment of the ramp rate dependence of  $T_g$  appears to be the most reasonable for investigating its relevance to the crystallization behavior because the crystallization tendency may be governed by the energy barrier of the molecular motion. However, because the crystallization is usually observed well above  $T_g$ , applicability of the fragility values determined by observing  $T_g$  may have limitation. A nice attempt to overcome this problem was made by Baird et al.,<sup>21</sup> in which viscosity of the melt was evaluated as a function of temperature to calculate fragility values, although the correlation with the crystallization tendency was not observed. Nevertheless, further efforts to investigate possible factors that influence crystallization are required because it is directly related to the formulation strategy for amorphous dosage forms.

### Relaxation During Rapid Cooling

Thermal analysis is the most common method for investigating the structural relaxation behavior of pharmaceutical glasses.<sup>24</sup> In general, spontaneous relaxation during storage is reproduced by intentional annealing to examine the relaxation process quantitatively, under the assumption that the recovery enthalpy observed in the DSC scan is equivalent to the relaxation enthalpy consumed during annealing. In this procedure, little or no relaxation is expected during the heating/cooling cycles in the thermal program. However, the growth of recovery peaks was observed for TLB with decreasing cooling rate, which indicates extremely high molecular mobility during the temperature scan. Figure 4 shows the enthalpy recovery of TLB as a function of cooling rate. Even when TLB

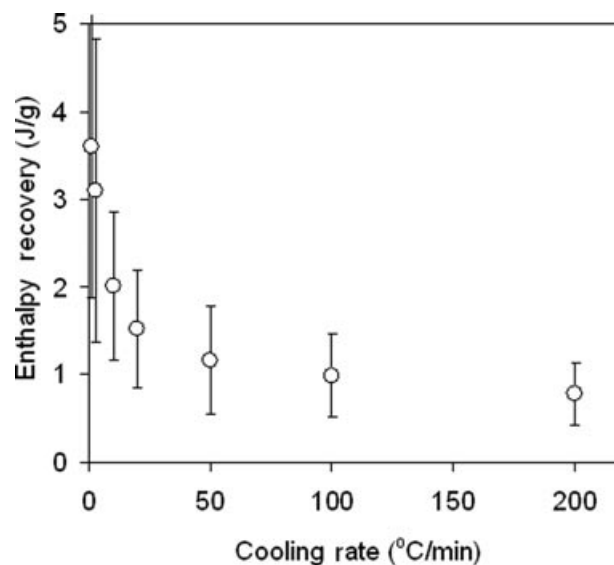


**Figure 4.** Enthalpy recovery of TLB as a function of the cooling rate.

was cooled at 100°C/s, an enthalpy recovery of approximately 1 J/g was observed, although the cooling process completed within 2 s. Because the heating process was also performed at 100°C/s, half of the enthalpy (~0.5 J/g) could be considered to be consumed in each (cooling and heating) process. The enthalpy of structural relaxation,  $H$ , can be described as a function of time,  $t$ , as follows:

$$H = H_0 \left[ 1 - \exp \left\{ - \left( \frac{t}{\tau} \right)^\beta \right\} \right] \quad 0 < \beta \leq 1 \quad (4)$$

where  $H_0$  stands for initial excess enthalpy with reference to metastable amorphous. The relaxation time,  $\tau$ , is regarded as a function of temperature. The fitting parameter,  $\beta$ , which may take values between 0 and 1, is usually regarded as a reflection of the relaxation time distribution; when  $\beta$  is near unity, the distribution is narrow, whereas a value of  $\beta$  much less than unity would indicate a broad distribution.  $H_0$  can be calculated from

$$H_0 = \Delta C_p (T_g - T) \quad (5)$$

where  $\Delta C_p$  is the heat capacity difference between the crystalline and the glassy states.  $\tau$  can be expressed by the Vogel–Tamman–Fulcher equation shown below:

$$\tau = \tau_0 \exp \left( \frac{DT_0}{T - T_0} \right) \quad (6)$$

where  $\tau_0$  is timescale of vibrational motions (ca.  $10^{-14}$  s).  $T_0$  is a constant that usually has almost the same value as the Kauzmann temperature. Figure 5 shows the relaxation times as functions of  $D$  and

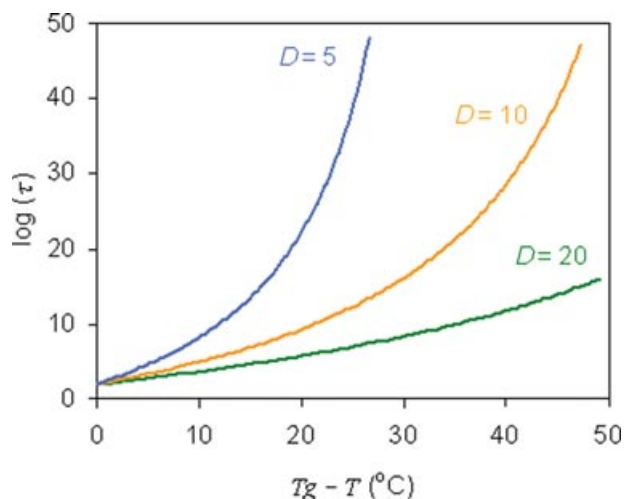


**Figure 5.** Model calculation of relaxation time as a function of temperature and the strength parameter,  $D$ .

temperature. The results demonstrate that smaller  $D$  provides rapid growth in relaxation time with decreasing temperature below  $T_g$ .

Figure 6 shows model calculations for the evolution of relaxation enthalpy obtained by integrating Eq. 4 numerically with time for various fragilities and ramp rates. Because the relaxation time increased dramatically with decreasing temperature when  $D$  has a low value, evolution of relaxation enthalpy should be very small for glasses with low  $D$  values. Also, relaxation is suppressed with rapid cooling. Note that the values obtained in this simulation should be an overestimation because the degree of relaxation in the glass transition region is usually much smaller than expected.<sup>21</sup> Nevertheless, the calculation indicates that a relatively large  $D$  value is required for the glasses that exhibit relaxation recovery in the high-speed DSC measurements because almost no relaxation is expected for fragile glasses ( $D < 10$ ). This contradicts the observation made for TLB and requires further investigation.

### Crystallization Tendency in Aqueous Media

Crystallization tendency of the drug in the dry state is closely related to the storage stability of the amorphous formulation. Meanwhile, crystallization tendency in aqueous media is an important factor that requires further clarification for improving oral absorption of poorly soluble drugs because the amorphous state must be maintained in gastric fluids to obtain a long supersaturation state.<sup>3-5</sup> Table 1 summarizes the crystallization behavior of various model drugs in the wet state with their basic physical characteristics. The order of each drug is presented according to the classification system proposed by Baird et al.<sup>13</sup> Class I drugs crystallize during cooling from the melt in the DSC analysis, class II drugs

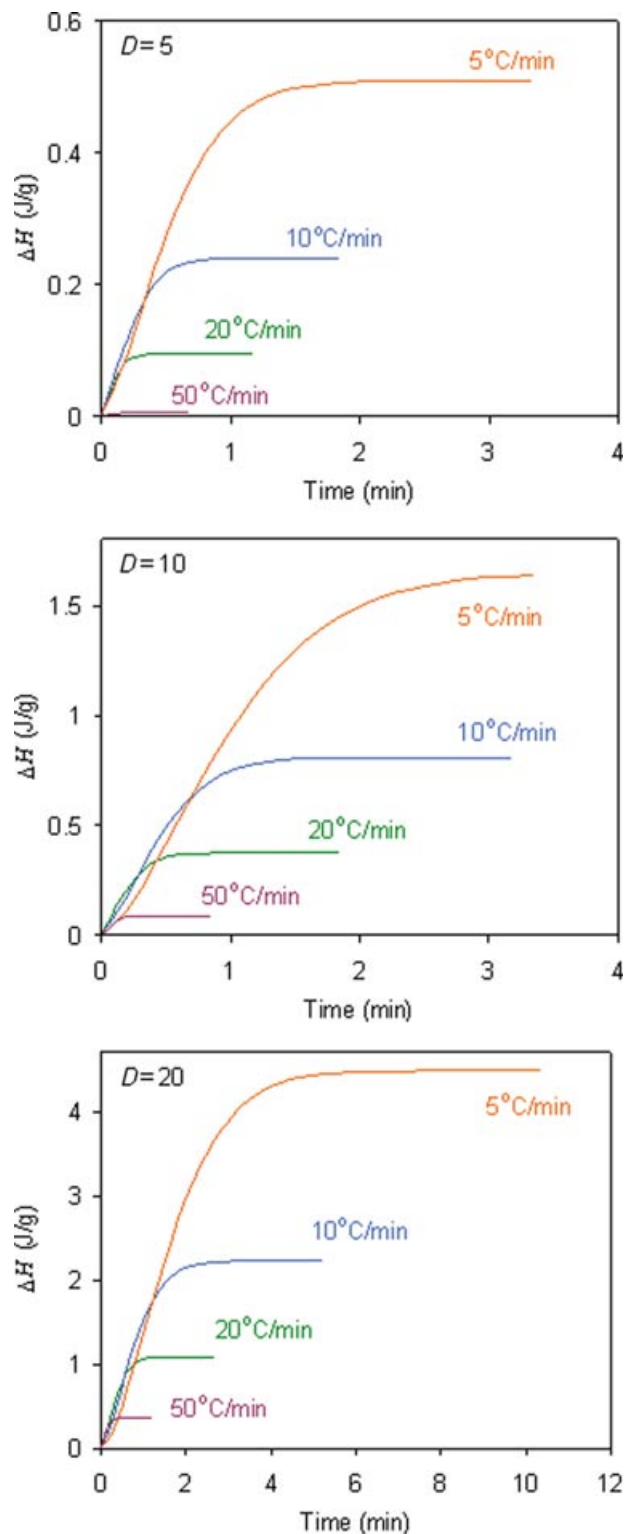


**Figure 6.** Time evolution of relaxation enthalpy during the DSC scan as a function of the ramp rate and the strength parameter,  $D$ .

maintain an amorphous state during the cooling but crystallize during subsequent heating, and class III drugs do not crystallize during the cooling/heating cycle mentioned above. It is obvious that classification



**Table 1.** Crystallization Tendency in the Presence of Water

Drug	Classification <sup>a</sup>	$T_m$ (°C)	$T_g$ (°C)	Solubility (mg/mL) <sup>b</sup>	$m^c$	Molecular State After 24 h
Carbamazepme	I	190	59	0.95	55.3	Crystallized <sup>d</sup>
Haloperidol	I	150	29	0.003	72.8 <sup>e</sup>	Crystallized <sup>d</sup>
Tolbutamide	I	127	20	0.11	101	Crystallized <sup>d</sup>
Acetaminophen	II	169	23	140	60	Crystallized
Flurbiprofen	II	115	-7	0.033	61	Crystallized
Nifecupine	II	172	45	0.0058	33	Amorphous
Fenofibrate	III	81	-18	0.1 <sup>f</sup>	76	Crystallized
Ibuprofen	III	75	-43	0.011	58	Crystallized
Indomethacin	III	160	46	0.004	58	Amorphous
Itraconazole	III	164	56	0.000001 <sup>g</sup>	731	Partially crystallized
Ketoconazole	III	147	42	0.08	78	Partially crystallized
Procaine	III	61	-39	1.3	69	Crystallized

<sup>a</sup>Classification system proposed by Baird et al.<sup>13</sup> For details, see the text.

<sup>b</sup>Aqueous solubility at room temperature. Data are taken from Ref. 25 unless otherwise mentioned.

<sup>c</sup>From Ref. 13 except for class I drugs.

<sup>d</sup>Already crystallized prior to contact with water.

<sup>e</sup>Fragility of the mesophase.

<sup>f</sup>From Ref. 26.

<sup>g</sup>From Ref. 27.

in the dry state has no relevance with crystallization tendency in the wet state. Some observations have indicated that solvent-mediated transformation is governed by solubility to the solvent and solvent–drug interactions.<sup>14,15</sup> The solubility threshold that results in solvent-mediated transformation is usually around 10 mM. Only acetaminophen satisfies this requirement. However, water is frequently an exceptional solvent because of its ability to form hydrogen bonds with drug molecules and transformation can be observed even though the solubility is far below the threshold, which was also of the case in this observation.

Interestingly, there is an indication that crystallization tendency in the wet state is correlated with  $T_g$  in the dry state. The model drugs with a  $T_g$  higher than room temperature maintained an amorphous state or crystallized only partially, whereas those with a  $T_g$  lower than that crystallized almost completely. Although the value of  $T_g$  itself is less meaningful in the wet state, it should be valid for assuming the order of molecular mobility under identical temperature conditions. Molecular mobility is sometimes correlated with the crystallization rate in the solid state<sup>28</sup>; however, this is not a general observation presumably due to strong restrictions on molecular diffusion. Existence of a solvent may aid rearrangement of the solid structure by decreasing energy barriers. As a result, the molecular mobility may become more dominant for controlling the crystallization behavior. The supersaturation mechanism requires further investigation because it is a complicated process that involves dissolution, supersaturation, crash out into a crystalline or amorphous state, and formation of nanoparticles.<sup>29</sup> Nevertheless,  $T_g$  of a drug may function as a parameter for assessing its supersaturation ability. Because the number of the compound used in

this study has been limited, further observation on this matter is required.

## CONCLUSIONS

Amorphous characteristics of drugs with high crystallization tendency, TLB, CBZ, and HPD, were investigated using high-speed DSC. TLB and CBZ were transformed into the amorphous state successfully by rapid cooling from the melts, whereas HPD formed the mesophase upon the cooling. No thermodynamic parameters of the glasses explained their low glass-forming ability. CBZ and HPD were found to form relatively strong glass and mesophase, respectively, and thus the general thought that glasses with low glass-forming ability are fragile did not hold. Also investigated was the correlation of thermodynamic parameters with crystallization tendency upon contact with water, which is important for evaluating *in vivo* efficacy of amorphous formulations.  $T_g$  was the best descriptor for assuming crystallization tendency upon contact with water.

## ACKNOWLEDGMENTS

This work was in part supported by World Premier International Research Center (WPI) Initiative on Materials Nanoarchitectonics, MEXT, Japan, and Low-carbon Research Network, Japan.

## REFERENCES

1. Kawakami K. 2009. Current status of amorphous formulation and other special dosage forms as formulations for early clinical phases. *J Pharm Sci* 98:2875–2885.
2. Murdande SB, Pikal MJ, Shanker RM, Bogner RH. 2010. Solubility advantage of amorphous pharmaceuticals: I. A thermodynamic analysis. *J Pharm Sci* 99:1254–1264.

3. Kawakami K. 2012. Modification of physicochemical characteristics of active pharmaceutical ingredients and application of supersaturatable dosage forms for improving bioavailability of poorly absorbed drugs. *Adv Drug Delivery Rev* 64: 480–495.
4. Vandecruys R, Peeters J, Verreck G, Brewster ME. 2007. Use of a screening method to determine excipients which optimize the extent and stability of supersaturated drug solutions and application of this system to solid formulation design. *Int J Pharm* 342:168–175.
5. Brouwers J, Brewster ME, Augustijns P. 2009. Supersaturating drug delivery systems: The answer to solubility-limited oral bioavailability? *J Pharm Sci* 98:2549–2572.
6. Sollohub K, Cal K. 2010. Spray drying technique: II. Current applications in pharmaceutical technology. *J Pharm Sci* 99:587–597.
7. Breitenbach J. 2002. Melt extrusion: From process to drug delivery technology. *Eur J Pharm Biopharm* 54:107–117.
8. Bhugra C, Pikal MJ. 2008. Role of thermodynamic, molecular, and kinetic factors in crystallization from the amorphous state. *J Pharm Sci* 97:1329–1349.
9. Caron V, Bhugra C, Pikal MJ. 2010. Prediction of onset of crystallization in amorphous pharmaceutical systems: Phenobarbital, nifedipine/PVP, and phenobarbital/PVP. *J Pharm Sci* 99:3887–3900.
10. Tarjus G, Kivelson SA, Nussinov Z, Viot P. 2005. The frustration-based approach of supercooled liquids and the glass transition: A review and critical assessment. *J Phys Condens Matter* 17:R1143–R1182.
11. Tanaka H. 2005. Two-order parameter model of the liquid-glass transition. I. Relation between glass transition and crystallization. *J Non-Cryst Solids* 351:3371–3384.
12. Shintani H, Tanaka H. 2006. Frustration on the way to crystallization in glass. *Nat Phys* 2:200–206.
13. Baird JA, van Eerdenbrugh B, Taylor LS. 2010. A classification system to assess the crystallization tendency of organic molecules from undercooled melts. *J Pharm Sci* 99:3787–3806.
14. Gu CH, Young Jr. V, Grant DJW. 2001. Polymorph screening: Influence of solvents on the rate of solvent-mediated polymorphic transformation. *J Pharm Sci* 90:1878–1890.
15. Kawakami K, Asami Y, Takenoshita I. 2010. Calorimetric investigation of solvent-mediated transformation of sulfamerazine polymorphism. *J Pharm Sci* 99:76–81.
16. Kawakami K. 2007. Reversibility of enantiotropically-related polymorphic transformations from a practical viewpoint: Thermal analysis of kinetically reversible/irreversible polymorphic transformations. *J Pharm Sci* 96:982–989.
17. Kawakami K. 2010. Parallel thermal analysis technology using an infrared camera for high-throughput evaluation of active pharmaceutical ingredients: A case study of melting point determination. *AAPS PharmSciTech* 11:1020–1205.
18. Kawakami K. 2011. Dynamics of ribavirin glass in sub- $T_g$  temperature region. *J Phys Chem B* 115:11375–11381.
19. Senkov ON. 2007. Correlation between fragility and glass-forming ability of metallic alloys. *Phys Rev B* 76:104202-1–104202-6.
20. Crowley KJ, Zografi G. 2001. The use of thermal methods for predicting glass-former fragility. *Thermochim Acta* 380:79–93.
21. Baird JA, Santiago-Quinonez D, Rinaldi C, Taylor LS. 2012. Role of viscosity in influencing the glass-forming ability of organic molecules from the undercooled melt state. *Pharm Res* 29:271–284.
22. Huang D, McKenna GB. 2001. New insights into the fragility dilemma in liquids. *J Chem Phys* 114:5621–5630.
23. Wang LM, Velikov V, Angell CA. 2002. Direct determination of kinetic fragility indices of glass-forming liquids by differential scanning calorimetry: Kinetic versus thermodynamic fragilities. *J Chem Phys* 117:10184–10192.
24. Kawakami K, Pikal MJ. 2005. Calorimetric investigation of the structural relaxation of amorphous materials: Evaluating validity of the methodologies. *J Pharm Sci* 94:948–965.
25. Yalkowsky SH, He Y. 2003. *Handbook of aqueous solubility Data*. Boca Raton, Florida: CRC Press, 2003.
26. Law D, Wang W, Schmitt EA, Qiu Y, Krill SL, Fort JJ. 2003. Properties of rapidly dissolving eutectic mixtures of poly(ethylene glycol) and fenofibrate: The eutectic microstructure. *J Pharm Sci* 92:505–515.
27. Peeters J, Neeskens P, Tollenaere J, Van Remoortere P, Brewster ME. 2002. Characterization of the interaction of 2-hydroxypropyl- $\beta$ -cyclodextrin with itraconazole at pH 2, 4, and 7. *J Pharm Sci* 91:1414–1422.
28. Aso Y, Yoshioka S, Kojima S. 2000. Relationship between the crystallization rates of amorphous nifedipine, phenobarbital, and flopropione, and their molecular mobility as measured by their enthalpy relaxation and  $^1\text{H}$  NMR relaxation times. *J Pharm Sci* 89:408–416.
29. Alonzo DE, Gao Y, Zhou D, Mo H, Zhang GGZ, Taylor LS. 2011. Dissolution and precipitation behavior of amorphous solid dispersions. *J Pharm Sci* 100:3316–3331.